

# [2] Radiance distribution simulation in a transparent medium with fresnel boundaries containing aluminum nanoparticles

Zvekov A.A., Nikitin A.P., Aduiev B.P.  
 Institute of Chemistry of Coal and Material Science SB RAS  
 Kalenskii A.V.  
 Kemerovo State University

## Abstract

The radiative transfer equation in a slab with Fresnel boundaries was solved with spherical harmonics method in the case of transparent medium containing aluminum nanoparticles. The computer program was developed, the angular radiance distribution on the slab boundaries and in the slab center were calculated. It was concluded that Fresnel boundary conditions make the angular distribution on the slab boundaries asymmetric. The utilization of angular radiance distribution for the reverse problems solution of the scattering systems spectroscopy was discussed.

**Keywords:** NANOPARTICLES, RADIATIVE TRANSFER EQUATION, SPHERICAL HARMONICS, FRESNEL BOUNDARY CONDITIONS.

**Citation:** ZVEKOV A.A. RADIANCE DISTRIBUTION SIMULATION IN A TRANSPARENT MEDIUM WITH FRESNEL BOUNDARIES CONTAINING ALUMINUM NANOPARTICLES / ZVEKOV A.A., KALENSKII A.V., NIKITIN A.P., ADUEV B.P. // COMPUTER OPTICS. – 2014. – VOL. 38(4). – P. 749-756.

## Introduction

Spectroscopy methods of scattering systems are widely applied in monitoring of natural and technical objects which can both dissipate and absorb the light. These problems can arise when sounding the atmosphere [1], analyzing biological [2] and food products [3], studying and optimizing solar cell batteries [4] and optical detonators [5-10], etc. When analyzing experimental results the most often used are diffusion approximation [11,12], Kubelka-Munk theory [11,13] and the radiative transfer equation using Monte-Carlo methods [14]. The reason for their prevalency is their relative simplicity (diffusion approximation and Kubelka-Munk theory) or accessibility of ready-made simulation codes (Monte Carlo methods). At the same time, diffusion approximation and Kubelka-Munk theory are applied only in the extreme case of a very strong light scattering [11] and only approximate boundary conditions may be identified for them [11]. As a result, their prognoses may result in significant errors [11,13].

Most papers on the radiative transfer theory have used Marshak boundary conditions [15] which may be applied as approximate conditions when considering the boundary, where the refraction index cannot be changed (clouds in atmosphere). This type of boundary conditions cannot be used in the case of systems where the refraction index

is changed at the boundary: colloids, metal nanoparticles dispersed in a transparent matrix, solar cells, etc. In this case it is necessary to identify Fresnel boundary conditions [16-19]. Solution of the radiative transfer equation with Fresnel boundary conditions using the discrete ordinate method was implemented in [17]. In paper [18] the radiance transfer simulation was executed in a solar energy concentrator in case of spherical and frame luminescent quantum dots. We have proposed in our paper [19] to adapt the spherical harmonics method to solution of the radiative transfer equation in a homogeneous slab calculating integral absorption indexes, and reflection and transmission coefficients. As an object we used some pressed polycrystalline samples of pentraerythrite tetranitrate (PETN) with nanoscale aluminum additives. Benchmarking of the theory and the experiment enabled to estimate the complex nanoparticle refraction index at the laser radiance wavelength of 643 nm [19]. Thus, application of the radiative transfer theory to specified objects is relevant for development of spectroscopic research methods. Most papers consider the integral characteristics such as the diffuse reflectance and transmission factors. Their use doesn't allow us to determine all unknown parameters of the scattering medium; it becomes necessary to use additional information about the system that reduces opportunities of

this method. In order to improve the information quality, we may use angular distribution of the reflected and transmitted light which was not considered in our previous paper [19].

Paper objective: the radiance angular distribution simulation of the transmitted and reflected light in the transparent medium containing metal nanoparticles. As a model system we used PETN samples containing aluminum nanoparticles of different radius. Selection of this system has been stipulated by the possibility to apply it as a detonable composition for optical detonators [5-10], as well as by the fact that the matrix material (PETN) can be compressed with obtaining a dense and optically transparent sample with no visible defects. Calculations have been performed at the wavelength of 1064 nm (the first harmonic of neodymium laser) that corresponds to initiation conditions of detonable compositions for optical detonators in experimental works [8-10].

**1. The spherical harmonics method with Fresnel boundaries**

Let us consider the transparent material slab wherein metal particles are uniformly distributed with a rather low concentration, so that their interaction may be neglected. Stationary distribution of unpolarized light in such system may be described by the radiative transfer equation which has the form [11]:

$$(\hat{\mathbf{i}}, \nabla)I(\mathbf{r}, \hat{\mathbf{i}}) = -kI(\mathbf{r}, \hat{\mathbf{i}}) + \frac{k\Lambda}{4\pi} \oint I(\mathbf{r}, \hat{\mathbf{i}}') \cdot x(\hat{\mathbf{i}}, \hat{\mathbf{i}}') d\hat{\mathbf{i}}' + q(\mathbf{r}, \hat{\mathbf{i}}) \quad (1)$$

where  $I(\mathbf{r}, \hat{\mathbf{i}})$  – is the light intensity in point  $r$  in  $\hat{\mathbf{i}}$  – direction,  $k$  – is the linear attenuation coefficient,  $\Lambda = k_{sca}/k$  – is the albedo of single interaction between light quantum and the scattering medium,  $x(\hat{\mathbf{i}}, \hat{\mathbf{i}}')$  – is the scattering indicatrix,  $q(\mathbf{r}, \hat{\mathbf{i}})$  – is the function of light sources. A left member of the equation has a meaning to change the intensity into  $\hat{\mathbf{i}}$  – direction when changing 3D coordinates. The first summand in the right part indicates the reason for intensity reducing, i.e. the light extinction; the second summand indicates the reason for its increasing due to its scattering, and the third member shows the intensity increase due to light sources located within the light scattering medium. Suppose that the beam broadening due to scattering processes is much smaller than the beam radius falling perpendicular to the top surface of the sample that enables to transfer to the one-dimensional problem. Taking into consideration these simplifications, the radiative transfer equation will take the following form [15,19]:

$$\left( \hat{\mathbf{i}} \cdot \frac{dI(x, \hat{\mathbf{i}})}{dx} \right) = -kI(x, \hat{\mathbf{i}}) + \frac{k\Lambda}{4\pi} \oint I(x, \hat{\mathbf{i}}') \cdot x(\hat{\mathbf{i}}, \hat{\mathbf{i}}') d\hat{\mathbf{i}}' \quad (2)$$

Proceeding to the dimensionless coordinate  $\tau = kx$  and introducing the spherical angle cosine  $\mu = \cos \theta$

between the direction of the beam initial incidence angle, which is perpendicular to the sample upper boundary, and the direction of interest, we reduce the equation (2) to the following form [15,19]:

$$\mu \frac{dI(x, \mu)}{d\tau} = -I(x, \mu) + \frac{\Lambda}{2} \int_{-1}^1 I(x, \mu') \cdot x(\mu, \mu') d\mu' \quad (3)$$

In order to solve the equation (3) we used the spherical harmonics method in which the angular distribution of light intensity was searched in the form of a superposition of spherical harmonics [15,19]. Since we neglect the light beam broadening and the dependence on the polar angle  $\phi$  is missing, the spherical harmonics may be replaced in terms of Legendre polynomials ( $P_l$ ):

$$I(x, \hat{\mathbf{i}}) = \sum_{l=0}^{\infty} \frac{2l+1}{2} C_l(x) \cdot P_l(\mu) \approx \sum_{l=0}^N \frac{2l+1}{2} C_l(x) \cdot P_l(\mu) \quad (4)$$

where  $N$  – is the maximum considered harmonics index,  $C_l$  – means expansion coefficients depending on coordinates. The scattering indicatrix may be arranged in terms of Legendre polynomials [15,19]:

$$x(\hat{\mathbf{i}}, \hat{\mathbf{i}}') = \sum_{l=0}^{\infty} \frac{2l+1}{2} x_l \cdot P_l(\mu, \mu') \approx \sum_{l=0}^N \frac{2l+1}{2} x_l \cdot P_l(\mu, \mu') \quad (5)$$

After we have converted the second member of equation (1) and applied recurrence relations for Legendre polynomials, the equation system for the intensity expansion coefficients will take the form [15,19]:

$$\frac{1}{2m+1} \cdot \left[ (m+1) \frac{dC_{m+1}}{d\tau} + m \frac{dC_{m-1}}{d\tau} \right] + \left( 1 - \frac{\Lambda x_m}{2} \right) C_m = 0 \quad (6)$$

Equation (6) is known as the spherical harmonics equation system. It is difficult to directly apply the equation system (6), since if take into consideration the boundary conditions which express the external radiation falling down to the sample, the angular distribution will be greatly extended in the direction of the initial beam. In order to avoid this disadvantage, it was suggested to deduct a part of the solution directly relating to the falling light  $I_0$  [15,19] and to calculate only the scattered component  $I_s$ :

$$I = I_0 + I_s \quad (7)$$

The non-scattered intensity component ( $I_0$ ) is reduced in accordance with the Bouguer law. Since in some cases we will study reasonably thin samples, the reflection from the sample's rear boundary shall be taken into consideration. Therefore, the non-scattered component of the solution will take the following form:

$$I_0 = J \cdot (\exp(-\tau) + R_f \exp(\tau - 2L)) \quad (8)$$

where  $J$  – is the density of radiation power penetrated through the sample,  $R_f$  – is the Fresnel reflection coefficient at normal beam incidence. The equation system for the scattered component is as follows:

$$\frac{1}{2m+1} \cdot \left[ (m+1) \frac{dC_{m+1}}{d\tau} + m \frac{dC_{m-1}}{d\tau} \right] + \left( 1 - \frac{\Lambda x_m}{2} \right) C_m = \frac{J\Lambda x_m}{2} \left[ \exp(-\tau) + (-1)^m R_f \exp(\tau - 2L) \right] \quad (9)$$

Let us identify the boundary conditions for the equation system (9). We will assume that particles are not directly on the sample surface. Then the interaction of light with the surface will be described by the Fresnel formulas [16-19]:

$$\begin{aligned} I_s(0, \mu) &= R(\mu) I_s(0, -\mu), \quad 0 \leq \mu \leq 1, \\ I_s(L, -\mu) &= R(\mu) I_s(0, \mu), \quad -1 \leq \mu \leq 0 \end{aligned} \quad (10)$$

where  $R(\mu)$  – is the angle dependence of the Fresnel reflection coefficient. The equations (10) give the conditions on the front and rear boundaries of the sample, respectively. They need to be converted into interactions of harmonics contributions on the surface. For this purpose we use the intensity expansion in terms of Legendre polynomials:

$$\begin{aligned} \sum_{m=0}^N \frac{2m+1}{2} C_m(0) P_m(\mu) &= \\ \sum_{m=0}^N \frac{2m+1}{2} (-1)^m C_m(0) \cdot P_m(\mu) \cdot R(\mu) \end{aligned} \quad (11)$$

By multiplying the equation by  $P_l(\mu)$  and integrating between 0 and 1 (angles fall into the medium), we'll get the following for the front and rear boundaries, respectively:

$$\begin{aligned} \sum_{m=0}^N (N_{lm} - R'_{lm}) C_m(0) &= 0 \\ \sum_{m=0}^N (\tilde{N}_{lm} - \tilde{R}'_{lm}) C_m(L) &= 0 \end{aligned} \quad (12)$$

where the matrix elements are as follows:

$$\begin{aligned} R'_{lm} &= (-1)^m \frac{2m+1}{2} \int_0^1 P_m(\mu) R(\mu) P_l(\mu) d\mu \\ N_{lm} &= \frac{2m+1}{2} \int_0^1 P_m(\mu) P_l(\mu) d\mu \\ \tilde{N}_{lm} &= (-1)^m N_{lm} \\ R'_{lm} &= (-1)^m \tilde{R}'_{lm} \end{aligned} \quad (13)$$

In accordance with the Fresnel formulas the angular dependence of the reflection coefficient at  $\mu \geq \sqrt{1-n^{-2}}$  is determined as follows:

$$\begin{aligned} R(\mu) &= \frac{1}{2} \left( \frac{\sqrt{n^{-2}-1+\mu^2}-\mu}{\sqrt{n^{-2}-1+\mu^2}+\mu} \right)^2 \times \\ &\times \left[ 1 + \left( \frac{\mu\sqrt{n^{-2}-1+\mu^2}-1}{\mu\sqrt{n^{-2}-1+\mu^2}+\mu^2+1} \right)^2 \right] \end{aligned} \quad (14)$$

Since the light is considered to be non-polarized, the equation (14) contains contributions of s- and p-polarization which correspond to the first and second members in square brackets, respectively. At  $\mu < \sqrt{1-n^{-2}}$  the total internal reflection is taking place and  $R(\mu) = 1$ .

The equation (9) may be presented in the following form:

$$C_m(\tau) = \sum_{l=0}^N a_{ml} \tilde{C}_l \exp(\gamma_l \tau) + C_p^1 \exp(-\tau) + C_p^2 \exp(\tau) \quad (15)$$

The last two terms are a particular solution of the non-homogeneous equation. The coefficients  $C_p^1$  and  $C_p^2$  equal to:

$$C_p^1 = -J\Lambda \cdot \sum_{m=0}^N [\delta_{pm} + A_{pm}]^{-1} B_m \quad (16)$$

$$C_p^2 = J\Lambda R_f \exp(-2L) \cdot \sum_{m=0}^N [\delta_{pm} - A_{pm}]^{-1} B_m$$

where

$$A_{pm} = - \left[ \frac{p+1}{2p+1} \delta_{p,p'+1} + \frac{p}{2p+1} \delta_{p,p'-1} \right]^{-1} \left[ \left( 1 - \frac{\Lambda x_m}{2} \right) \delta_{p'm} \right]$$

and

$$B_m = \left[ \frac{m+1}{2m+1} \delta_{m,m'+1} + \frac{m}{2m+1} \delta_{m,m'-1} \right]^{-1} \left[ \frac{x_{m'}}{2} \right]$$

The degree “-1” means to take the inverse matrix from the matrix, the elements of which are shown in square brackets; the matrix multiplication operation is performed between multipliers in square brackets.

The first right summand (15) corresponds to the solution expansion by private vectors of the matrix  $A_{pm}$  (matrix  $a_{ml}$ ) with respective spectral numbers (eigen values)  $\gamma_l$ . The expansion coefficients  $\tilde{C}_l$  shall be determined in terms of the boundary conditions (10). These boundary conditions form the system consisting of  $2N+2$  equations, from which  $2N$  are linearly independent. The number of determined coefficients equals to  $N+1$ , i.e. the system is overdetermined. Therefore, we used minimization of the sum of squared deviations (SSD) of values in left parts (10) from zero. As a result, we get the following equation for coefficients written in a matrix form:

$$\tilde{C} = - \left[ (Z\tilde{a})^T (Z\tilde{a}) \right]^{-1} (Z\tilde{a})^T (ZC_p) \quad (17)$$

where  $Z = \begin{pmatrix} N - R' \\ \tilde{N} - \tilde{R}' \end{pmatrix}$ ,  $\tilde{a} = \begin{pmatrix} a \\ a \cdot \exp(-\gamma L) \end{pmatrix}$ ,  $C_p = \begin{pmatrix} C_p^1 \\ C_p^2 \end{pmatrix}$ .

An alternative approach to determine coefficients  $\tilde{C}_l$  involves the application of matrix singular value decomposition  $Z$  [20]. This method also provides a sat-

isfactory approximation but it means an arbitrary rule when excluding small eigen values which can affect the result accuracy.

The scattering medium parameters were calculated using the Mie theory [5-7,9,21,22] regarding aluminum nanoparticles as spherical. This theory allows us to calculate both absorption and scattering cross sections and the scattering indicatrix. The complex metal refraction index for the wavelength of 1064 nm (the first harmonic of neodymium laser) was  $0.96 - 8.07i$  [23], the matrix refraction index was equal to 1.54. The number of harmonics used in calculations was determined based on the anisotropy of the scattering indicatrix. The more indicatrix anisotropy, the greater number of harmonics is to be used for its correctly describing and obtaining reliable results. The maximum radius of aluminum nanoparticles in our calculations was 700 nm that resulted to the strongly anisotropic scattering indicatrix, for the approximation of which we used  $N = 31$ . With less number of harmonics the angular component attained an oscillating structure which disappeared when increasing the number of harmonics. Similar calculation characteristics were noted also by other authors [24].

## 2. Computer implementation

For computer implementation of the solution of the radiative transfer equation using the spherical harmonics method in the slab with Fresnel boundaries a special software package has been developed. According to the statement of the problem the calculations were performed for the transparent medium containing metal nanoparticles. As software input parameters we used the radius of metal nanoparticles, the light wavelength, the complex metal refraction index and the transparent medium refractive index at the same wavelength, the material slab thickness, densities of metal and the transparent medium, and a mass fraction of metal nanoparticles.

The software package included the following major components:

1. Calculating the absorption and scattering efficiency factors, as well as the scattering indicatrix within the framework of the Mie theory for the specified nanoparticle radius and material.
2. Calculating the linear absorption and scattering coefficients at the specified nature, mass fraction and radius of metal nanoparticles. Determination of the single scattering albedo. Approximation of the scattering indicatrix in terms of Legendre polynomials.
3. Calculating the matrices of coefficients in the spherical harmonics equation system (9), the matrices of the boundary conditions (14), the matrices of coefficients in equations (15)-(16) describing the radiative transfer equation solved in terms of derivatives, and the specific

solution of the nonhomogeneous equation.

4. Solving the matrix equations (12) using the formula (17) and determining the homogeneous equation solution expansion coefficients by eigenvectors in terms of Fresnel boundary conditions.

5. Calculating the angular distribution of the radiation intensity in defined points, graphing the calculated dependencies, and calculating the slab transmission and reflection.

In order to test the software the test calculation has been performed for distribution of the radiation energy absorbed at  $Q_{sca} = 1.0$ ,  $Q_{abs} = 0.01$ . In this parameter region the light scattering diffusion mode shall be observed [11], where the observed dimensionless absorption index should be close to  $\sqrt{3 \cdot (1 - \Lambda)}$ . The obtained value of the observed dimensionless absorption index amounts to 0.1775 and differs by 3% from the predicted theoretical value that may testify to the calculation correctness.

## 3. Results and discussion

Fig. 1 and 2 show the results of simulation of the angular dependence of reflected and transmitted light for the samples containing aluminum nanoparticles of different radius with the mass fraction of 0.05%. As a direction from which the angle is to be measured out, we have identified the direction of incidence perpendicular to the front sample surface. We defined the sample thickness equal to the extinction length multiplied by 4 in order to obtain comparable results. Let us consider the main features of the angular dependencies obtained. In case of reflected light the intensity distribution has a sloping minimum within  $\theta < 0.2\pi$  (the direction is into the sample's interior perpendicular to the front surface) with further increase up to a nearly stationary value. For large particle radiuses we can further observe the increase until the maximum occurs at  $\theta = \pi$ .

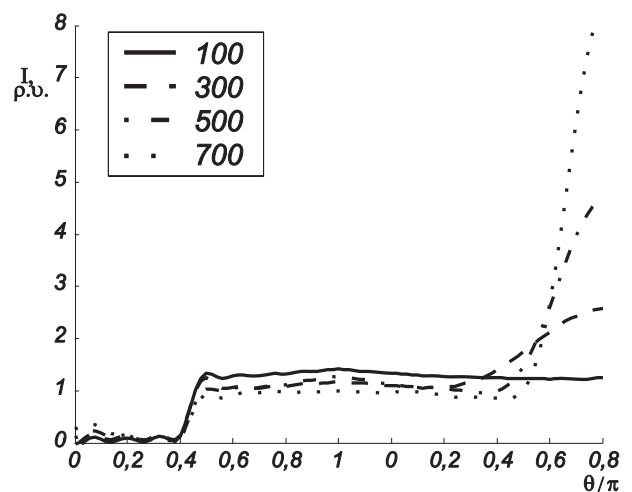


Fig. 1. Angular intensity distribution in reflected light

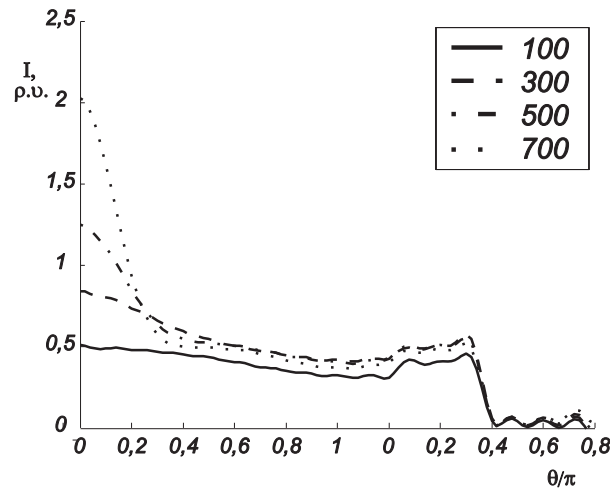


Fig. 2. Angular intensity distribution in transmitted light

These features depend on two reasons, i.e. the Fresnel dependence of the light reflection index on the incidence angle and the scattering anisotropy factor. The Fresnel dependence of the reflection index with the used medium refraction index is shown in Fig. 3. Within the incidence angles  $0.23\pi \geq \theta \geq \pi$  the reflection index is equal to one, i.e. the total internal reflection takes place. The boundary transmission sharply increases and the reflection index decreases by 6.7 times when varying the incidence angle from  $0.225\pi$  to  $0.2\pi$ . It decreases more thereafter and becomes minimum at  $\theta=0$  and equal to  $(n-1)^2/(n+1)^2 = 0.045$ . Comparing Fig. 1 and Fig. 3 we recognize that the increase in the reflected light intensity takes place in the same range of incidence angles that the increase of the reflection index.

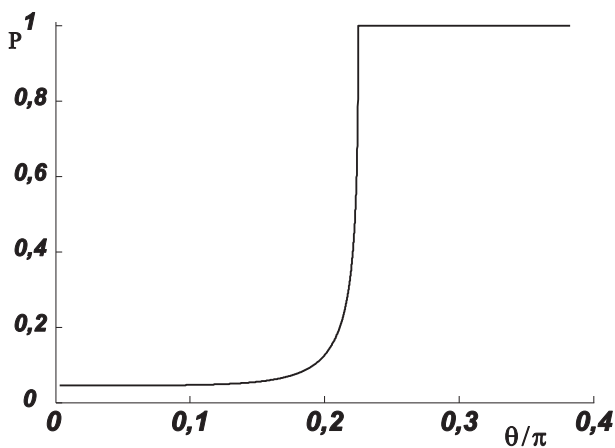


Fig. 3. Dependence of the reflection index on the incidence angle

Let us compare this characteristic of the angular distribution with those ones obtained by other authors. As an example, we consider the paper [12] in which the angular distribution of the scattered radiation has been calculated in diffusion approximation at different light incidence angles on an infinite flat-parallel slab of the scattering, but not absorbing, medium. It is shown in [12] that in case of normal light incidence the angular distribution is symmetrical within the surface. The higher the angle of incidence (in respect to a surface vertical alignment), the more asymmetrical distribution is; moreover, the asymmetry degree is reduced while increasing thickness of the scattering slab. The reason is that when having a thin slab, the single scattering prevails, and when having a thick slab – the multiple with “erasing memory” of the original direction.

We have examined in our calculations only the case of normal radiation incidence on the scattering medium and, in contrast to paper [12], the asymmetrical angular distribution has been found. The asymmetry of the intensity angular distribution is related to the angular dependence of the Fresnel reflection coefficient which wasn't discussed in paper [12]. It should also be noted that diffusion approximation cannot be used to solve the radiative transfer equation with Fresnel boundary conditions. The diffusion approximation is equivalent to using only two terms of intensity expansion of interaction in terms of Legendre polynomials in (4). This approximation doesn't allow accurately estimate the dependence of the light reflection coefficient on the boundary using the same interaction. Therefore, inaccurate

boundary conditions based on the energy conservation law which don't take into consideration the angular dependence are always applied in diffusion approximation [11,12].

Influence of the anisotropy factor is demonstrated by the sharp increase of the reflected light intensity at  $\theta \approx \pi$ . As the radius of nanoparticles increases, the anisotropy factor which is equal to the cosine of the average scattering angle  $g = \langle \cos \theta \rangle$  decreases from -0.185 to -0.945. So the larger the radius of nanoparticles, the more radiation is reflected in the opposite direction. This characteristic is reflected not only on intensity angular dependences at the boundaries, but also inside of the sample. Fig. 4 shows the example of the intensity angular distribution in the center. Dependencies calculated for large-radius nanoparticles have two local max values at  $\theta \approx 0$  and  $\theta \approx \pi$  which are related to the dominating scattering direction. In case of low-radius nanoparticles (100 nm), these local max values are not observed, and the intensity-angle dependence is very weak.

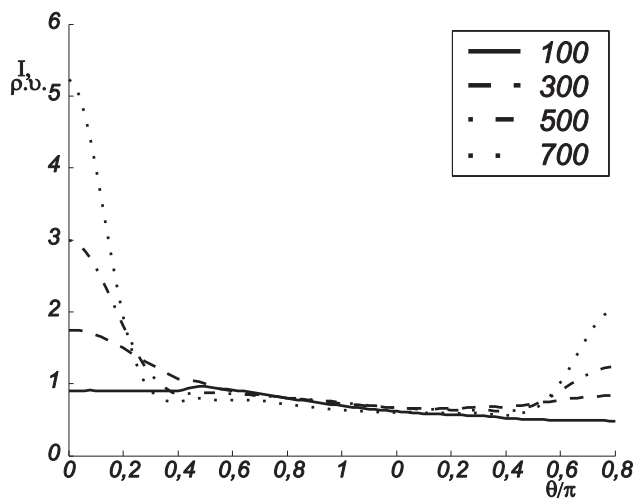


Fig. 4. Intensity angular distribution in the sample's center

In physics of light scattering systems we often use a concept of the Lambertian surface, i.e. the surface in which the intensity reflection is the same in all directions. According to Fig. 1, the radiative intensity doesn't practically depend on the angle within the range of  $0.24\pi \leq \theta \leq \pi$  in case of small-radius aluminum nanoparticles that relates to low light scattering anisotropy. Thus, if the light scattering anisotropy is small, regardless of Fresnel boundary conditions the reflection of the wide scattering medium will be close to isotropic. Increase or decrease of the anisotropy factor will lead to still greater devi-

ations from the Lambert surface approximation. Let us consider the informative value of the radiation angular distribution in solving the inverse problem. We have previously identified in paper [19] the optical properties of aluminum nanoparticles in the medium with Fresnel boundaries using a photometric integrating sphere. Based on experimental reflection and transmission coefficients measured in accordance with the sample thickness and the mass fraction of aluminum nanoparticles (average radius is 50 nm), the complex aluminum refractive index was determined. As follows from the results of this work, the main parameter influencing the radiation angular distribution at the sample boundary is the anisotropy factor of the scattering indicatrix. Therefore, it is reasonable to experimentally determine the intensity angular dependence if the strongly anisotropic scattering is expected.

### Conclusion

The paper has considered the solution of the radiative transfer equation in the scattering medium slab with Fresnel boundaries using the spherical harmonics method. We used as example the propagation of light in the dielectric medium containing aluminum nanoparticles. The basic blocks of the developed software have been identified in order to simulate the radiative transfer.

The angular intensity distributions have been calculated at the slab center and boundaries. It has been concluded that Fresnel boundary conditions may result to the asymmetric angular intensity distribution within the slab boundaries. It is shown that in case of the strongly anisotropic scattering indicatrix the intensity distribution on sample surfaces is extended in the direction of a normal line oriented from the surface into the environment that may be used to solve inverse problems of spectroscopic measurements of light scattering systems.

### Acknowledgments

The work has been performed with support of the RFBR (the Russian Foundation for Basic Research) (grant No. 14-03-00534 A), grant of the President of the Russian Federation (grant no. MK-4331.2015.2), and the Ministry of Education and Science of the Russian Federation (NIR no. 3603 on the government contractual work no. 64/2014).

## References

- 1. Kochikov, I.V.** Numerical procedures for substances identification and concentration calculation in the open atmosphere by processing a single ftir measurement / I.V. Kochikov, A.N. Morozov, I.L. Fufurin // *Computer Optics*. – 2012. – Vol. 36(4). – P. 554-561. (In Russian).
- 2. Lisenko, S.A.** Noninvasive Fast Analysis of Hemoglobin Levels in Blood Using a Fiber Optic Spectrophotometer / S.A. Lisenko, M.M. Kugeiko, V.A. Firago, A.N. Sobchuk // *Journal of Applied Spectroscopy*. – 2014. – Vol. 81(1). – P. 118-126.
- 3. Rey, J.M.** Photothermal diffuse reflectance: a new tool for spectroscopic investigation in scattering solids / J.M. Rey, J. Kottman, M.W. Sirgist. // *Applied Physics B*. – 2013. – Vol. 112. – P. 547-551.
- 4. Moulin, E.** Improved light absorption in thin-film silicon solar cells by integration of silver nanoparticles / E. Moulin, J. Sukmanowski, P. Luo, R. Carius, F.X. Royer, H. Stiebig // *Journal of Non-Crystalline Solids*. – 2008. – Vol. 354. – P. 2488-2491.
- 5. Aduiev, B.P.** Explosive decomposition of PETN with nanoaluminum additives under the influence of pulsed laser radiation at different wavelengths / B.P. Aduiev, D.R. Nurmukhametov, R.I. Furega, A.A. Zvekov, A.V. Kalenskii // *Russian Journal of Physical Chemistry B*. – 2013. – Vol. 7(4). – P. 453-456.
- 6. Ananyeva, M.V.** Promising compounds for the cap of optical detonator / M.V. Ananyeva, A.A. Zvekov, I.Yu. Zykov, A.V. Kalensky, A.P. Nikitin // *Perspektivnye materialy – Advanced mater.* – 2014. – Vol. 7. – P. 5-12. (In Russian).
- 7. Kalenskii, A.V.** Spectral dependencies of the critical energy density of petn containing nickel nanoparticles composites laser initiation / A.V. Kalenskii, M.V. Anan'eva, A.A. Zvekov, I.Yu. Zykov // *Basic Problems of Material Science*. – 2014. – Vol. 11(3). – P. 340-345. (In Russian).
- 8. Aduiev, B.P.** Effect of ultrafine Al-C particle additives on the PETN sensitivity to radiation exposure / B.P. Aduiev, D.R. Nurmukhametov, V.P. Tsipilev, R.I. Furega // *Combustion, Explosion, and Shock Waves*. – 2013. – Vol. 49(2). – P. 215-218.
- 9. Aduiev, B.P.** Effect of the initial temperature on the threshold of laser initiation of pentaerythritol tetranitrate seeded with aluminum nanoparticles / B.P. Aduiev, G.M. Belokurov, D.R. Nurmukhametov // *Russian Journal of Physical Chemistry B*. – 2012. – Vol. 6(4). – P. 511-516.
- 10. Aduiev, B.P.** Photosensitive material based on PETN mixtures with aluminum nanoparticles / B.P. Aduiev, G.M. Belokurov, D.R. Nurmukhametov, N.V. Nelyubina // *Combustion, Explosion, and Shock Waves*. – 2012. – Vol. 48(3). – P. 361-366.
- 11. Ishimaru, A.** *Electromagnetic Wave Propagation, Radiation, and Scattering*. – New Jersey: Prentice Hall. 1st edition. – 1990.
- 12. Gao, M.** Angular distribution of diffuse reflectance from incoherent multiple scattering in turbid media / M. Gao; X. Huang; P. Yang; G.W. Kattawar // *Applied Optics*. – 2013. – Vol. 52(24). – P. 5869-5879.
- 13. Sandoval, C.** Deriving Kubelka–Munk theory from radiative transport / C. Sandoval, A.D. Kim // *Journal of Optical Society of America A*. – 2014. – Vol. 31(3). – P. 628-636.
- 14. Hayakawa, C.K.** Comparative analysis of discrete and continuous absorption weighting estimators used in Monte Carlo simulations of radiative transport in turbid media / C.K. Hayakawa, J. Spanier, V. Venugopalan // *Journal of Optical Society of America A*. – 2014. – Vol. 31(2). – P. 301-311.
- 15. Budak, V.P.** *Methods of radiative transfer equation solution*. – Moscow: Izdatelskii dom MEI. – 2007. (In Russian).
- 16. Garcia, R.D.M.** Radiative transfer with polarization in a multi-layer medium subject to Fresnel boundary and interface conditions / R.D.M. Garcia // *Journal of Quantitative Spectroscopy & Radiative Transfer*. – 2013. – Vol. 115. – P. 28-45.
- 17. Garcia, R.D.M.** Fresnel boundary and interface conditions for polarized radiative transfer in a multilayer medium / R.D.M. Garcia // *Journal of Quantitative Spectroscopy & Radiative Transfer*. – 2012. – Vol. 113. – P. 306-317.
- 18. Sahin, D.** Radiative transport theory for light propagation in luminescent media / D. Sahin; B. Ilan // *Journal of Optical Society of America A*. – 2013. – Vol. 30(5). – P. 813-820.
- 19. Aduiev, B.P.** A study into optical properties of aluminum nanoparticles in pentaerythritol tetranitrate with photometric sphere / B.P. Aduiev, D.R. Nurmukhametov, G.M. Belokurov, A.A. Zvekov, A.V. Kalenskii, A.P. Nikitin, I.Yu. Liskov // *Technical physics*. – 2014. – Vol. 59(9). – P. 1387-1392.
- 20. Liemert, A.** Green's functions for the two-dimensional radiative transfer equation in bounded media / A. Liemert, A. Kienle // *Journal of Physics A: Math. Theor.* – 2012. – Vol. 45 – P. 175201-175210.
- 21. Shifrin, K.S.** *Light scattering in turbid medium*. – Moscow, Leningrad: Gos. izd. tekhniko-teoreticheskoy lit. – 1951. (In Russian).
- 22. Asenchik, O.D.** Application of the scattered field technique for ftd modeling of electromagnetic fields near dielectric and metallic nanoparticles / O.D. Asenchik, E.G. Starodubtsev // *Computer Optics*. – 2013. – Vol. 37(3). – P. 316-325. (In Russian).
- 23.** *Optic constants of natural ant technical media: hand book* / edited by V.M. Zolotarev, V.N. Morozov, E.V. Smirnova Leningrad: Himiya. – 1984. (In Russian).

**24. Budak, V.P.** On the solution of a vectorial radiative transfer equation in an arbitrary three-dimensional turbid medium with anisotropic scattering / V.P. Budak, S.V. Korkin // Journal of Quantitative Spectroscopy & Radiative Transfer. – 2008. – Vol. 109. – P. 220-234.

